

Study on the influence of thermal characteristics of transmission components on overload control of grid-connected lines of wind farms

Zhiyu Sheng¹, Shihao Wang¹, Yimin Yin¹, Jingran Wang², and Mengxia Wang^{1,*}

¹EDP Sciences, Editorial Department, 91944 Les Ulis Cedex A, France | Key Laboratory of Power System Intelligent Dispatch and Control Ministry of Education (Shandong University), Jinan, Shandong Province, 250061, China

²State Grid Jibei Electric Power Company Ltd

Abstract. The rapid growth of the installed capacity of wind power is not coordinated with the planning and development of the power grid, which may lead to transmission line overload when N-1 failure occurs in grid-connection lines of large-scale wind power. However, the existing overload protection and stability control strategies cannot adapt to this short-term power flow overload, so a large number of wind turbines need to be removed, which is brought the accommodation problem of large scale cluster wind power. The grid-connection line of wind farms has significant non-synchronization (thermal inertia) between current-carrying and temperature changes, and the short-term current-carrying potential needs to be tapped. This paper summarizes the thermal balance models of two kinds of transmission components and explores the influence of thermal characteristics of transmission components on the overload control of grid-connected lines of wind farms. The simulation results show that considering the thermal inertia of transmission components in overload control can significantly reduce the cut of wind power, fully tap the overload capacity of grid-connection lines.

1 Introduction

With the rapid development of new energy power generation technique, the cumulative installed capacity of wind power in the world continues to increase. In China, the number has reached 210 GW at the end of 2019, which significantly increased by more than 13% compared to 2018^[1]. Compared with the rapid increase of wind power installed capacity, the expansion of power grid relatively lags behind due to the longer construction period and higher investment.

From the point of view of the grid construction, the lack of transfer capability of grid-connected lines of wind farms is becoming one of the important restrictive factors for wind power integration. If the capability of grid-connected lines can be improved, the absorption

* Corresponding author: wangmx@sdu.edu.cn

capacity of wind power will be greatly improved. The dynamic thermal rating (DTR) technique^[2] are recognized as effective solutions. Traditionally, the transfer capability of an overhead conductor is represented by its static thermal rating (STR), which is calculated under the assumption of conservative weather conditions around the conductor. Thus, STR tends to underestimate the transfer capability of the conductor in most times. To this issue, dynamic thermal rating (DTR) technique is proposed in 1977^[3], which can calculate the thermal rating based on the real-time metering weather conditions around the conductor. As reported, the application of DTR technique is capable of increasing the transmission line rating by 10% to 30% compared with STR during 90% of the time. In [4], the benefits brought by the application of DTR technique on a wind farm. The results show that the number of turbines into operation is 45 units, and compared with 32 units which is calculated under STR of transmission lines, the wind power utilization is increased by 40.6%. In [5], the existing power transmission lines used a DTR system to instead of broadly-used static rating. The result showed that the dynamic thermal rating allowed more line capacity than static rating, and the optimal size of wind farm was approximately triple when using DTR comparing to the static rating. In [6], a protection relay is designed, which realizes the purpose of eliminating the overload of grid-connected lines by combining DTR technology and protection control. However, in many cases, DTRs may underestimate the thermal load capacity of transmission components because of ignoring the thermal inertia effect of the conductor. The fluctuation of wind power will make the thermal inertia of grid-connection lines' temperature become more significant. If the temperature of grid-connected lines can be taken as the limit on process overload control, the load-carrying capacity of transmission components may be further improved on the basis of the DTR technique. Therefore, based on the output fluctuation characteristics of wind farms, the influence of thermal characteristics of transmission components on overload control of grid-connection lines is analysed in this paper.

2 Thermal model of transmission components

2.1 Thermal model of overhead conductor

The thermal behaviour of the overhead conductor is determined by its current and environmental conditions. Under the assumption that the transmission line is a uniform conductor, according to IEEE standard^[7], the heat balance equation of an overhead conductor can be expressed as:

$$\frac{dT_c}{dt} = \frac{1}{mC_p}(q_l + q_s - q_c - q_r) \quad (1)$$

where q_l represents the joule heating of the overhead line. q_s is the solar heating of the overhead line. q_c and q_r represent the convective cooling and the radiative cooling respectively. T_c represents the temperature of grid-connected lines. t is the operating time, m is the mass of the unit transmission line, and C_p is the specific heat capacity of the transmission line. When the load current of grid-connection lines and weather conditions along the line has been given, calculation equations of q_l , q_s , q_c and q_r can be expressed as :

$$\begin{cases} q_l = I_i^2 R(T_c) \\ R(T_c) = \frac{R(T_{max}) - R(T_{max})}{T_{max} - T_{low}} * (T_c - T_{low}) + T_{low} \end{cases} \quad (2)$$

$$q_s = \alpha Q_{se} \sin(\theta) A' \quad (3)$$

$$\begin{cases} q_{c1}(T_C) = [1.01 + 0.0372(\frac{D\rho_f V_w}{\mu_f})^{0.52}] k_f k_{angle} (T_C - T_a) \\ q_{c2}(T_C) = 0.0119(\frac{D\rho_f V_w}{\mu_f})^{0.6} k_f k_{angle} (T_C - T_a) \\ q_{c3}(T_C) = 0.0205 \rho_f^{0.5} D^{0.75} (T_C - T_a)^{1.25} \end{cases} \quad (4)$$

$$q_r(T_{max}) = 0.0178 D \varepsilon [(\frac{T_{max} + 273}{100})^4 - (\frac{T_a + 273}{100})^4] \quad (5)$$

where $R(T_C)$ is the resistance of per unit length conductor under T_C (Ω/m), $[T_{low}, T_{max}]$ is the range of the linear resistance-temperature relationship; D is the diameter of the conductor, ε is the heat radiation coefficient of the conductor, A' is the projection area of the per unit length conductor (mm^2). The parameters D , ε and A' are all related to the type of the conductor; q_{c1} and q_{c2} are used to calculate the heat losses caused by the low wind speed and the high wind speed under T_{max} , respectively. q_{c3} is used to calculate the natural convective heat loss under zero wind speed under T_C ; Q_{se} is the solar radiation on the per unit square ground (W/m^2); ρ_f is the air density (kg/m^3), μ_f is the air viscosity ($Pa \cdot s$), θ is the incidence of solar radiation ($^\circ$); T_a is the ambient temperature around the conductor ($^\circ C$); V_w is the wind speed (m/s), k_{angle} is the wind direction factor that is related to the angle between the wind direction and the conductor. The differential term on the left side of formula (1) of the imperative formula is equal to 0. According to the IEEE standard, the static thermal rating (STR), $I_{max,o}$, of the overhead conductor can be calculated by:

$$I_{max,o} = \sqrt{\frac{q_c(T_{max}) + q_r(T_{max}) - q_s}{R(T_{max})}} \quad (6)$$

where T_{max} represents the maximum allowable temperature of the conductor ($^\circ C$), T_{max} is set to $70^\circ C$ in this paper.

If the temperature can be used as the constraint of the capacity of grid-connected lines, the lack of transfer capability of the grid-connected lines of wind farms can be solved, and the utilization rate of wind power can be improved. In this paper, the implicit trapezoidal method is used to discretize the differential equation of the dynamic heat balance equation, which realizes one-step iteration and avoids the problem of data accuracy overflow in the calculation process. The discrete dynamic heat balance equation can be expressed as:

$$T_{C(t)} = T_{C(t-\Delta t)} + \frac{\Delta t}{2mC_p} \begin{bmatrix} q_l(T_{C(t-\Delta t)}) + q_s(T_{C(t-\Delta t)}) \\ -q_c(T_{C(t-\Delta t)}) - q_r(T_{C(t-\Delta t)}) \\ +q_l(T_{C(t)}) + q_s(T_{C(t)}) \\ -q_c(T_{C(t)}) - q_r(T_{C(t)}) \end{bmatrix} \quad (7)$$

where $T_{C(t)}$ represents the temperature of grid-connected lines at time t . Δt represents the differential step. The meaning of q_l , q_s , q_c and q_r has been specifically described above.

2.2 Thermal model of XLPE insulated power cable

XLPE insulated cable has the characteristics of high mechanical strength, excellent insulation and corrosion resistance, so it is suitable for submarine laying^[8]. In comparison with the overhead conductor, power cables have a relatively complex structure with multiple layers. Figure 1 shows the equivalent circuit of a typical XLPE insulated cable^[9].

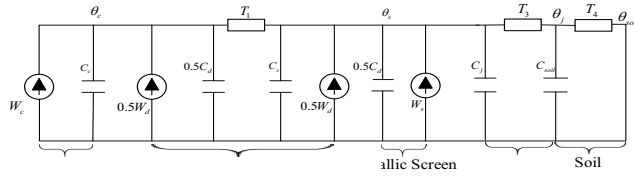


Fig. 1. Equivalent thermal circuit of the XLPE cable.

In figure 1, W_c , W_d and W_s is respectively conductor loss, insulating dielectric loss and metallic screen loss. θ_c , θ_s , θ_j and θ_{soil} respectively is conductor temperature, metallic screen temperature, jacket temperature and soil temperature. C_c , C_d , C_j and C_{soil} respectively represents conductor heat capacity, insulating dielectric heat capacity, metallic screen heat capacity, jacket heat capacity and soil heat capacity. T_1 , T_3 and T_4 respectively is thermal resistance of insulating dielectric, thermal resistance of jacket and thermal resistance of soil.

According to the thermal-electrical analogy, the heat balance equations of XLPE insulated power cable can be expressed as:

$$\begin{cases} (C_c + 0.5C_d) \frac{d\theta_c}{dt} = -\frac{1}{T_1}\theta_c + \frac{1}{T_1}\theta_s + (W_c + 0.5W_d) \\ (0.5C_d + C_s) \frac{d\theta_s}{dt} = \frac{1}{T_1}\theta_c - \left(\frac{1}{T_1} + \frac{1}{T_3}\right)\theta_s + \frac{1}{T_3}\theta_j + (0.5W_d + W_s) \\ C_{soil} \frac{d\theta_j}{dt} = \frac{1}{T_3}\theta_s - \left(\frac{1}{T_3} + \frac{1}{T_4}\right)\theta_j + \frac{1}{T_4}\theta_{soil} \end{cases} \quad (8)$$

In figure 1, the heat produced by the joule loss of the conductor, the insulating dielectric loss, and the metallic screen loss (per unit length) of the cable can be calculated using equations (9) – (11), respectively, as follows:

$$W_c = I^2 \times r_{20} [1 + \alpha(\theta_c - 20)] = I^2 \times r \quad (9)$$

$$W_d = U_\varphi^2 \omega C \tan \delta \quad (10)$$

$$W_s = \lambda_1 W_c = (\lambda'_1 + \lambda''_1) W_c \quad (11)$$

where I is Current of the cable. r_{20} is the conductor resistance at the reference temperature of 20°C. α is resistance-temperature coefficient. r is the conductor resistance after considering the temperature effect. U_φ is the voltage of the connected phase. ω is the angular frequency. C is the phase capacitance of cable. $\tan \delta$ is the tangent of dielectric loss angle of insulating dielectric. About the thermal resistance and heat capacity in the thermal balance model of cable. The calculation method of loss coefficient and other parameters is described in detail in IEC standard^[10-12].

In thermal steady state, the differential term on the left side of the equal sign of equation (8) is 0, $I^2 r$ and $\lambda_1 W_c$ are respectively replaced by W_c and W_s , and put $\theta = \theta_{max}$ (θ_{max} is the maximum long-term allowable operating temperature of the cable) into equation 8, simultaneous equations (9) to (11) can deduce the calculation formula of long-term allowable ampacity, $I_{max.c}$, of cable, which can be expressed as:

$$I_{max.c} = \sqrt{\frac{\theta_{max} - \theta_{soil} - W_d(0.5T_1 + T_3 + T_4)}{r[T_1 + (1 + \lambda_1)(T_3 + T_4)]} \quad (12)$$

As with overhead conductors, if the thermal inertia of cables is taken into account, the differential term of equation 8 cannot be taken as 0. If the implicit trapezoidal method is still used to discretize the differential equation of the dynamic heat balance equation, the discrete dynamic heat balance equation of XLPE insulated power cable can be expressed as:

$$\begin{cases} \theta_{e(t)} = \theta_{e(t-\Delta t)} + \frac{h}{2} \left[\begin{aligned} & -\frac{1}{C_1 T_1} \theta_{e(t-\Delta t)} + \frac{1}{C_1 T_1} \theta_{s(t-\Delta t)} + \frac{1}{C_1} (W_{e(t-\Delta t)} + W_{d1(t-\Delta t)}) \\ & -\frac{1}{C_1 T_1} \theta_{e(t)} + \frac{1}{C_1 T_1} \theta_{s(t)} + \frac{1}{C_1} (W_{e(t)} + W_{d1(t)}) \end{aligned} \right] \\ \theta_{s(t)} = \theta_{s(t-\Delta t)} + \frac{h}{2} \left[\begin{aligned} & \frac{1}{C_3 T_3} \theta_{e(t-\Delta t)} - \left(\frac{1}{C_3 T_3} + \frac{1}{C_3 T_3} \right) \theta_{s(t-\Delta t)} + \frac{1}{C_3 T_3} \theta_{j(t-\Delta t)} + \frac{1}{C_3} (W_{s(t-\Delta t)} + W_{d2(t-\Delta t)}) \\ & + \frac{1}{C_3 T_3} \theta_{e(t)} - \left(\frac{1}{C_3 T_3} + \frac{1}{C_3 T_3} \right) \theta_{s(t)} + \frac{1}{C_3 T_3} \theta_{j(t)} + \frac{1}{C_3} (W_{s(t)} + W_{d2(t)}) \end{aligned} \right] \\ \theta_{j(t)} = \theta_{j(t-\Delta t)} + \frac{h}{2} \left[\begin{aligned} & \frac{1}{C_4 T_4} \theta_{s(t-\Delta t)} - \left(\frac{1}{C_4 T_4} + \frac{1}{C_4 T_4} \right) \theta_{j(t-\Delta t)} + \frac{1}{C_4 T_4} \theta_{soil(t-\Delta t)} + \\ & \frac{1}{C_4 T_4} \theta_{s(t)} - \left(\frac{1}{C_4 T_4} + \frac{1}{C_4 T_4} \right) \theta_{j(t)} + \frac{1}{C_4 T_4} \theta_{soil(t)} \end{aligned} \right] \end{cases} \quad (13)$$

where $C_1 = C_c + 0.5C_d$, $C_3 = C_s + 0.5C_d$, $C_4 = C_{soil} \cdot \Delta t$ represents the differential step.

3 Results of comparison between overload control with temperature excitation and traditional overload control

In the traditional overload control, in order to ensure the grid-connection line safe steady operation, the thermal load limit of the grid-connection line is usually the maximum allowable ampacity (Determined by equations (6) and (12)) given by the design department. The aim is to convert the temperature constraint into a current constraint and make the value constant in the operation of the system. However, in the real-time operation environment, the real thermal ampacity of grid-connection lines is determined according to the real-time environmental conditions. The analysis shows that the change of conductor temperature shows the characteristic of inertia lag with the change of current or environmental condition. That is, the current and temperature of the conductor is a dynamic corresponding relationship, which also determines that the thermal ampacity of grid-connection lines, which is limited by temperature, is a dynamic capacity. The maximum allowable ampacity of grid-connection lines varies with different time. In the 1980s, the DTR technique began to be used in engineering practice and has been extended to the power utilities in many countries as a mature technique in the 1990s^[13-15]. After that, the DTR technique has been improved by integrating more advanced monitoring and communication techniques^[16-17], and now the DTR technique is capable of comprehensively metering the conductor temperature, mechanical state (stress and sag) and the micrometeorological conditions of the overhead line^[18]. Based on thermal characteristics of transmission components, the overload control of grid-connection lines of wind farms is simulated and analysed in this paper. The grid-connection line of onshore wind farms is overhead conductor and offshore wind farms is XLPE insulated power cable. Output power of wind farms in one hour are shown in figure 2

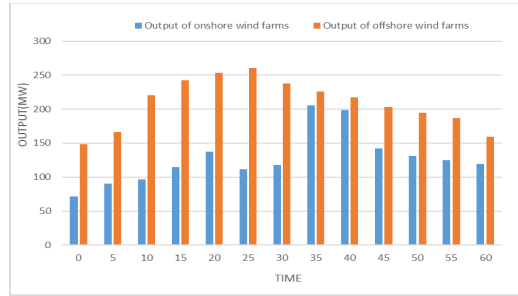


Fig. 2. Output power of wind farms.

It can be seen from figure 2, compared with output power of onshore wind farms, output power of offshore wind farms has the characteristics of high wind energy density and high annual utilization hours. In order to ensure the power supply reliability of the power grid, the parallel operation mode is adopted for the grid-connection lines, in which the type of onshore wind power transmission line is LGJ-300/40; and the cable cross section selected for the offshore wind power transmission line is 400mm². Suppose one of the grid-connection line withdrew from the time due to failure and lasted for 1 hour. In this section, the temperature change process of the grid-connection line and output power of wind farms on traditional overload control and overload control with temperature excitation which is monitored by the DTR technique are simulated respectively. Figure 3 and figure 4 are simulation results of onshore wind farms and offshore wind farms respectively.

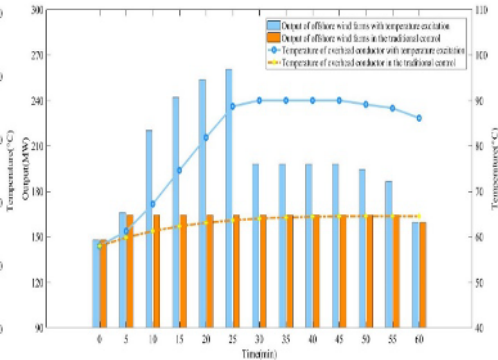
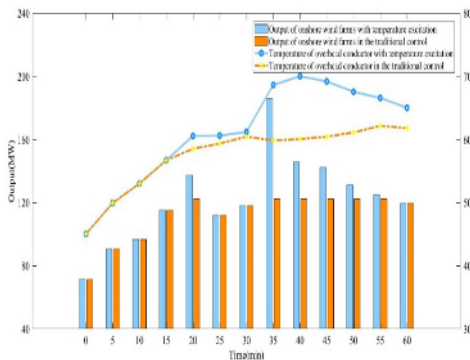


Fig. 3. Simulation results of onshore wind farms. **Fig. 4.** Simulation results of offshore wind farms.

It can be seen from figure 3 that when one of grid-connection lines is out of operation, another line will bear the overload of power flow transfer in this period. The load current of the line jumps to 2 times that of the original, which is larger than the maximum allowable ampacity, I_{max} (among which, the maximum allowable ampacity of overhead conductor, $I_{max,o}$, is 648A and the maximum allowable ampacity of cable, $I_{max,c}$, is 778A in this paper). For onshore wind farms, within 1 hour after N-1 failure, the current of the overhead line exceeds the static thermal rating after 15 min, and the overhead line cannot transport more wind energy under the traditional overload control, so the wind abandonment behavior begins to exist in the wind field after 15min to meet the static thermal constraint of the overhead conductor. Within one hour after N-1 failure, temperature of overhead conductors did not exceed 70°C until 40min. Therefore, in the overload control of overhead conductor with temperature excitation, abandonment of wind power did not occur until 40min and lasted only 5 minutes. Compared with the traditional overload control, the overload control with temperature excitation that is under the

monitoring of the DTR technique is limited by the temperature of overhead conductor, which gives play to the load capacity contained in the thermal dynamic process of overhead conductor to a certain extent, greatly reduces the cut of wind power. In this example, 132891 $kw\cdot h$ more wind power is accepted than the traditional overload control.

Similarly, for offshore wind farms, the current of XLPE insulated cable is always higher than its static thermal rating within 1 hour, so under the traditional overload control, in order to meet the constraint of cable static thermal rating, the abandonment behavior of offshore wind field exists all the time, and the volume of abandoned wind power is very large. However, the cable has the same thermal inertia as the overhead line, and its thermal inertia is more significant. Although the current is always higher than the static thermal rating, its temperature rises slowly until the 30min exceeds the maximum allowable temperature of 90 °C. Therefore, when overload control with temperature excitation of the cable, abandonment of wind power did not occur until 40min and lasted only 5 minutes. 507803 $kw\cdot h$ of wind power is accepted more than traditional overload control. To sum up, compared with the traditional overload control, if overload control is with temperature excitation, the load capacity contained in the thermal dynamic process of the transmission components will be brought into full play to a certain extent, and the power generation efficiency of the wind power will be increased. The utilization of wind energy will also be improved.

4 Results of comparison between overload control with temperature excitation and considering thermal characteristics of transmission components on process overload control

In the overload control with temperature excitation, the control will operate only when the temperature of the grid-connected line reaches the maximum allowable temperature. However, due to the thermal characteristics of transmission components, there is a slow change process for the temperature of grid-connected lines to reach the maximum. If the thermal characteristics of transmission components can be fully considered in the process of overload control, and small-scale control can be carried out before the temperature of the grid-connected line is about to reach the maximum, then the situation that the temperature exceeds the maximum value may be avoided. In this section, the temperature change process of the grid-connection line and output power of wind farms on overload monitored with temperature excitation and process overload control considering thermal characteristics of transmission components are simulated respectively. Figure 5 and figure 6 are simulation results of onshore wind farms and offshore wind farms respectively.

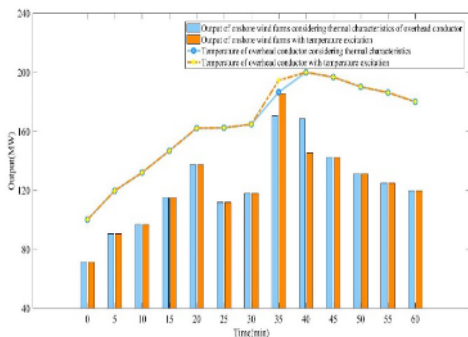


Fig. 5. Simulation results of onshore wind farms.

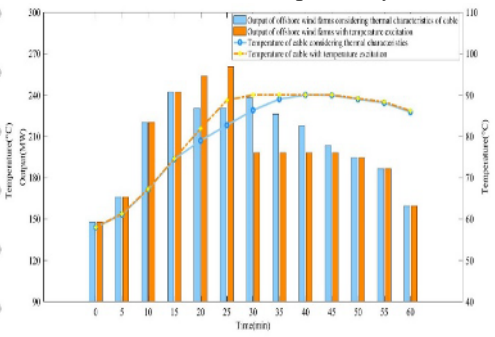


Fig. 6. Simulation results of offshore wind farms.

The bar graph in the figure shows output power of wind farms, and the broken line graph shows temperature change trajectory of the grid-connection line. It can be seen from figure 5 that when the thermal characteristics of transmission components are combined in the process of overload control of onshore wind farms, in 35min, although the temperature of the grid-connected line is not more than 70°C, it is also close to the limit and has an upward trend. In order to prevent large-scale wind abandonment caused by a substantial temperature limit, a small number of wind turbines will be removed predictably. In 40min, although the temperature of the grid-connected line still exceeds the limit, only a small number of wind turbines need to be removed to make the temperature of overhead line meet the thermal limit. For the overload control with temperature excitation, the control will act only when the temperature of the grid-connection line which is metered by DTR exceeds 70°C, so the behaviour of wind power curtailment starts at 40min. However, in order to reduce the temperature of the overhead conductor as soon as possible, the volume of wind power curtailment is much larger. Overall, considering the overload control of the thermal characteristics of transmission components, the volume of wind power curtailment in the whole process is 8000 $kW\cdot h$ less than overload control with temperature excitation.

Similarly, for offshore wind farms, the volume of wind power curtailment on overload control, which is considering the thermal inertia of cables, is also less than overload control with temperature excitation. In addition, because the thermal inertia of the cable is more significant, the wind farm starts wind power curtailment after 15min. Temperature of cable is greater than 90°C after 30min. Compared with overhead conductors, the start time of cable wind power curtailment is earlier, and the duration of cable wind power curtailment under the two overload controls is longer and the volume of wind power curtailment is less. Therefore, the process overload control considering the thermal characteristics of transmission components can greatly improve the transmission capacity of offshore wind power. To sum up, if the thermal characteristics of transmission components are taken into account in the process overload control, and predictive intervention and control are carried out in the control, the significant thermal inertia of the outgoing line can be brought into full play, and its load capacity can be brought into full play. The utilization rate of wind power is further improved.

5 Conclusion

Due to the strong fluctuation of wind power and the uncoordinated development between power grid construction and wind farm construction planning, the transmission capacity of grid-connection lines is insufficient and massive wind power curtailment is a problem during overload control. Aiming at this problem, this paper analyses the influence of the thermal characteristics of transmission components of wind farms on overload control of grid-connection lines. The heat balance model of overhead conductor and XLPE insulated cable are studied. Through the simulation of overload control of onshore wind farms and offshore wind farms, it is found that combining the thermal characteristics of transmission components in overload control can further give play to the short-term current carrying capacity of transmission lines, effectively reduce the volume of wind power curtailment of traditional overload control with static thermal rating as the limiting condition, and solve the problem of lagging power grid planning and development. At the same time, compared with the overload control with temperature excitation, the process overload control considering the thermal characteristics of transmission components makes more in-depth use of the thermal inertia of the grid-connection line, so as to further reduce the volume of wind power curtailment. As the thermal inertia of the cable is more significant, the effect is more significant.

This work was supported by the Science and Technology Project of State Grid Jibei Electric Power Company Ltd under Grant 52010119006U.

References

1. National Energy Administration 2019 Operation aspect of grid connected wind power
2. A R Ghahnavieh and M F Firuzabad, and M Othman 2015 Optimal unified power flow controller application to enhance total transfer capability IET Gener. Transm. Distrib vol 9 no 4 pp 358–368
3. B P Bhattarai et al 2018 Improvement of transmission line ampacity utilization by weather-based dynamic line rating IEEE Trans. Power Del vol 33 no 4 pp 1853–1863
4. Y L Wang 2019 Analysis on the DTR of Transmission Lines to Improve the Utilization of Wind Power 2018 IEEE Industry Applications Society Annual Meeting (IAS)
5. M A H Colin and J A Pilgrim 2019 Cable Thermal Risk Estimation for Overplanted Wind Farms IEEE Transactions on Power Delivery vol 35 pp 609-617
6. A K Kazerooni and J Mutale and M Perry and S Venkatesan and D Morrice 2011 Dynamic thermal rating application to facilitate wind power integration IEEE Trondheim PowerTech
7. 2007 IEEE Standard for Calculating the Current-Temperature of Bare Overhead Conductors IEEE Power Engineering Society NY USA pp c1-59.
8. ZHANG Jianmin and ZHANG Hongliang and XIE Shuhong et al 2017 Typical application and development prospect of XLPE insulated submarine cable for offshore wind farm in China Southern Power System Technology
9. R Olsen and J Holboell and U S Gudmundsdottir 2013 Electrothermal coordination in cable-based transmission grids IEEE Trans. Power Syst vol 28 no 4 pp 4867–4874
10. 2006 IEC Standard-Electric Cables-Calculation of the current rating-part 1-1:Current Rating Equations (100% load factor) and Calculation of Losses-General IEC Standard 60287-1-1
11. 2006 IEC Standard-Electric Cables-Calculation of the current rating-part 2-1:Thermal Resistance-Calculation of Thermal Resistance IEC Standard 60287-2-1
12. S C E Jupe and D Kadar and G Murphy and M G Bartlett and K T Jackson 2011 Application of a dynamic thermal rating system to a 132kV distribution network in Proc. 2nd IEEE PES Int. Conf. Exhibit. Innovative Smart Grid Technol pp 1–8.
13. S D Kim and M M Morcos 2013 An application of dynamic thermal line rating control system to up-rate the ampacity of overhead transmission lines IEEE Transactions on Power Delivery vol 28 no 2 pp 1231-1232
14. Q P Zhang and Z Y Qian 2005 Study on real-time dynamic capacity-increase of transmission line Power System Technology vol 29 no 19 pp 18-21
15. J S The and C M Lai and Nor Asiah Muhamad 2018 Prospects of using the dynamic thermal rating system for reliable electrical networks: A review IEEE Access vol 6 pp 26765-26778
16. K Morozovska and P Hilber 2017 Study of the monitoring systems for dynamic line rating Energy Proc. vol. 105 pp 2557–2562
17. Jiashen Teh and Ching-Ming Lai 2019 Reliability impacts of the dynamic thermal rating system on smart grids considering wireless communications IEEE Access vol 7 pp 41625 - 41635

18. Working Group on Monitoring & Rating of Subcommittee 15.11 on Overhead Lines
2013 Real-time overhead transmission-line monitoring for dynamic rating IEEE
Transactions on Power Delivery vol 31 no 3 pp 921-927